Available online at www.sciencedirect.com
SCIENCE DIRECT®
ELSEVIER
Current Applied Physics 3 (2003) 163–169
Current Applied Physics
Physics, Chemistry and Materials Science
www.elsevier.com/locate/cap

All-optical logic gates with bacteriorhodopsin

C.P. Singh, Sukhdev Roy *

Department of Physics and Computer Science, Dayalbagh Educational Institute (Deemed University) Dayalbagh, Agra 282005, India

Abstract

All-optical logic gates with bacteriorhodopsin (bR) protein molecules have been demonstrated based on all-optical switching of a cw probe laser beam by multiple pulsed pump laser beams due to nonlinear intensity-induced excited-state absorption. A cw probe laser beam at 640 nm corresponding to the peak absorption of O-state in the bR photocycle is switched by a pulsed pump laser beam at 570 nm corresponding to the maximum initial B state absorption, at relatively low powers. The switching characteristics have been used to design all-optical NOT and the universal NOR and NAND logic gates and the effect of various parameters such as variation in pump pulse width, pump intensity, lifetime of O state and absorption cross-section of the B state at probe wavelength on the switching characteristics has been analyzed.

PACS: 42.79.Ta; 42.65.−k; 87.14.Ee; 42.65.Pc
Keywords: All-optical switching; Optical computing; Nonlinear optics; Bacteriorhodopsin; Bio-molecular electronics

1. Introduction

Recent years have witnessed dramatic progress in investigating novel nonlinear materials for the design of all-optical devices for ultrafast high bandwidth communication and computing [1]. Current interest has focused on the design of all-optical molecular devices that offer number of advantages of small size and weight, high intrinsic speed, extremely low propagation delay and power dissipation and the ability to tailor properties to suit specific applications [2–4].

The photochromic protein bacteriorhodopsin (bR) contained in the purple membrane fragments of *Halobacterium halobium*, has emerged as an excellent material for bio-molecular photonic applications due to its unique advantages [3,4]. It exhibits high quantum efficiency of converting light into a state change, large absorption cross-section and nonlinearities, robustness to degeneration by environmental perturbations, high stability towards photo-degradation and temperature, response in the visible spectrum, low production cost, environmental friendliness, capability to form thin films in polymers and gels and flexibility to tune its kinetic and spectral properties by genetic engineering techniques, for device applications [3–7].

By absorbing green–yellow light, the wild type bR molecule undergoes several structural transformations in a complex photocycle that generates a number of intermediate states. The main photocycle of bR is as shown in Fig. 1. After excitation with green–yellow light at 570 nm, the molecules in the initial B state get transformed into J state with in about 0.5 ps. The species in the J state thermally transforms in 3 ps into the intermediate K state which in turn transforms in about 2 μs into the L state. From the L state bR thermally relaxes to the M^{I} state within 8 μs and undergoes irreversible transition to the M^{II} state. The molecules then relax through the N and O intermediates to the initial B state within about 10 ms. An important feature of all the intermediate states is their ability to be photo-chemically switched back to the initial B state by shining light at a wavelength that corresponds to the absorption peak of the intermediate in question. The wavelength in nm of the absorption peak of each species is shown as a subscript in Fig. 1.

Numerous applications have been proposed for bR. Its properties of proton pumping [6,7] and photo-electricity have been used for instance in desalination of seawater, conversion of sunlight to electricity [8,9], ultrafast light detection, chemo- and bio-sensing [10], artificial retinas [11], photon counters and photo-voltaic

* Corresponding author.
E-mail address: sukhdevr@hotmail.com (S. Roy).

1567-1739/02/$ - see front matter
doi:10.1016/S1567-1739(02)00195-5

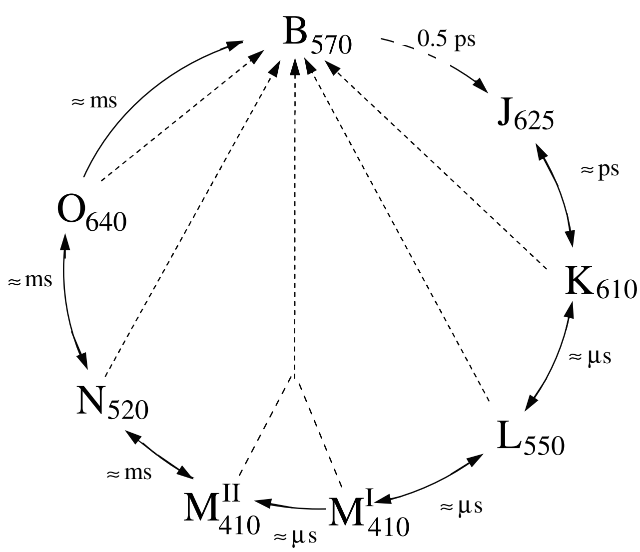

Fig. 1. Schematic of the photochemical cycle of bR molecule. Subscripts indicate absorption peaks in nm. Solid and dashed arrows represent thermal and photo-induced transitions respectively.

converters [12]. Its photo-chromic property has resulted in applications that include pattern recognition systems [13], information recording, associative and three dimensional memories [3,4], holography [14,15], second harmonic generation [16], saturable absorption, wave mixing and phase conjugation [17], nonlinear optical filtering [18], optical bistability [19], mode locking [20], spatial light modulation [18,21–24], optical image processing [25], neural networks [26], incoherent to coherent conversion [27,28], optical displays [29], optical computing [30], logic gates [31–34], beam deflection [35] and as a natural efficient photonic crystal [36].

Logic gates are the basic building blocks of digital computers. These gates (switches) have two stable states often referred to as logic 0 and logic 1. Computers encode information in terms of these two logic states or bits. For all-optical information processing, light addressed logic gates are of primary importance. An AND gate with bR has been proposed using sequential photoexcitation [31]. All-optical AND and OR logic gates with bR have been proposed based on a degenerate four wave mixing geometry [32]. Recently, all-optical logic gates using bR have also been shown based on complementary suppression-modulated transmission [33,34]. In both these approaches the designs have been based on a simplified two state model considering the steady state response that is applicable only when the M state has a very long lifetime. For digital optical computing we need to consider a pulsed operation, where time dependent analysis of all the intermediate states becomes necessary for an accurate analysis [32,37–39].

In this paper, we present a design of an all-optical inverter (NOT) and the universal NOR and NAND logic gates with bR based on all-optical switching of a cw probe laser beam by pulsed pump beams due to nonlinear intensity induced excited state absorption [37–39]. The switching dynamics have been analyzed using the rate equation approach considering a six state model of the bR photocycle. The effect of various parameters such as the pump pulse width, pumping intensity, life time of O state and absorption cross-section of the B state at probe wavelength on the switching characteristics has been analyzed.

2. Theoretical model

We introduce a simplified level diagram shown in Fig. 2 to represent the photochemical cycle of bR molecules, which enables adoption of the simple rate-equation approach for the population densities in the various intermediate states. The J state has been neglected in this simplified model, since it has an extremely short lifetime of 3 ps compared to the other states. A single M state (for both spectroscopically identical M^I and M^{II} states) and forward transitions between different intermediate states have been considered [40,41].

We consider bR molecules exposed to a light beam of intensity I'_m, which modulates the population densities of different states through the excitation and de-excitation processes that can be described by the rate equations in the following form [2,3,22,42]:

$$\frac{d\mathbf{N}}{dt} = \hat{O}\mathbf{N} \tag{1}$$

where operator $\hat{O}$ is defined in terms of the photo-induced and thermal transitions of different levels as

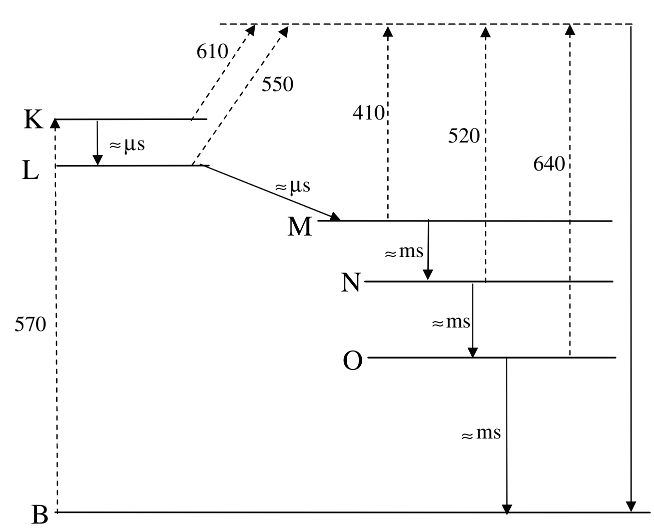

Fig. 2. Simplified level diagram representing the photochemical cycle of bR molecule. The solid and dashed arrows have the same meaning as in Fig. 1.

Table 1
Typical values of rate constants and absorption cross-sections

Rate constant	Value (s^{-1})	Absorption cross-section	Value (cm^2)	
			570 nm	640 nm
		σ_B	2.4×10^{-16}	0.3×10^{-16}
k_K	5.0×10^5	σ_K	1.8×10^{-16}	1.4×10^{-16}
k_L	2.0×10^4	σ_L	1.5×10^{-16}	...
k_M	1.0×10^3	σ_M	0.0	...
k_N	3.3×10^2	σ_N	1.7×10^{-16}	...
k_O	2.0×10^2	σ_O	1.1×10^{-16}	2.5×10^{-16}

$$\hat{O} = \begin{pmatrix} -I_m\sigma_B\psi_{BK} & I_m\sigma_K\psi_{KB} & I_m\sigma_L & I_m\sigma_M & I_m\sigma_N & k_O + I_m\sigma_O \\ 0 & k_K & -(k_L + I_m\sigma_L) & 0 & 0 & 0 \\ I_m\sigma_B\psi_{BK} & -(k_K + I_m\sigma_K\psi_{KB}) & 0 & 0 & 0 & 0 \\ 0 & 0 & k_L & -(k_M + I_m\sigma_M) & 0 & 0 \\ 0 & 0 & 0 & k_M & -(k_N + I_m\sigma_N) & 0 \\ 0 & 0 & 0 & 0 & k_N & -(k_O + I_m\sigma_O) \end{pmatrix} \tag{2}$$

and the transpose of the population vector **N** is given by

$$\tilde{N} = (N_B, N_K, N_L, N_M, N_N, N_O) \tag{3}$$

where σ and k are the absorption cross-sections and rate constants respectively of different states denoted by the respective subscripts, $\psi_{BK} = \psi_{KB} = 0.64$ are the quantum efficiencies for the transitions $B \rightarrow K$ and $K \rightarrow B$ respectively and I_m is the photon density flux of the modulation laser beam i.e. ratio of the intensity I'_m to the photon energy hν. The typical values of the constants and absorption cross-sections for various levels at different wavelengths are given in Table 1 [3,4,20,22,24,42].

Assuming optically thin bR samples, the propagation effects on the modulating light beams can be neglected in the following analysis. The modulating pump laser pulses for two input logic gates configurations such that the four input combinations (0,0), (0,1), (1,0) and (1,1) in terms of phase differences of their peaks can be considered, are given by

$$I'_{m1} = I'_{m0}\left[\exp\left(-c\left(\frac{t-t_{m1}}{\Delta t}\right)^2\right) + \exp\left(-c\left(\frac{t-t_{m2}}{\Delta t}\right)^2\right)\right]$$

and

$$I'_{m2} = I'_{m0}\left[\exp\left(-c\left(\frac{t-t_{m3}}{\Delta t}\right)^2\right) + \exp\left(-c\left(\frac{t-t_{m2}}{\Delta t}\right)^2\right)\right] \tag{4}$$

where t_{m1}, t_{m2} and t_{m3} are the times at which pulse maximum occurs, c is the pulse profile parameter and Δt is the pulse width.

We consider a cw probe laser beam of intensity I'_p ($I'_p \ll I'_m$) at 640 nm corresponding to the absorption maximum of the intermediate O state. The transmission of this signal is modulated by ground state absorption of bR by a pulsed pump laser beam at 570 nm corresponding to its peak absorption and by the excited state absorption of O state. The absorption spectra of the intermediate states indicates substantial absorption by B, K and O states at 640 nm [4,42]. Thus the nonlinear intensity dependent absorption coefficient α_p for the probe beam is written as

$$\alpha_p(I_m) = N_B(I_m)\sigma_{Bp} + N_K(I_m)\sigma_{Kp} + N_O(I_m)\sigma_{Op} \tag{5}$$

where the subscript p denotes the value at probe wavelength.

The propagation of the probe beam through the bR medium is governed by

$$\frac{dI_p}{dx} = -\alpha_p(I_m)I_p \tag{6}$$

where x is the distance in the medium and I_p is the intensity of the probe beam.

3. Results and discussion

The optical switching characteristics, namely the variation in the normalized transmitted intensity of the probe laser beam with time have been computed by solving the rate equations for the intermediate states through computer simulations using Eqs. (1)–(6) and the typical values of the rate constants and absorption cross-sections given in Table 1, with pump pulse width $\Delta t = 7$ ms, film thickness of 30 μm and peak pumping

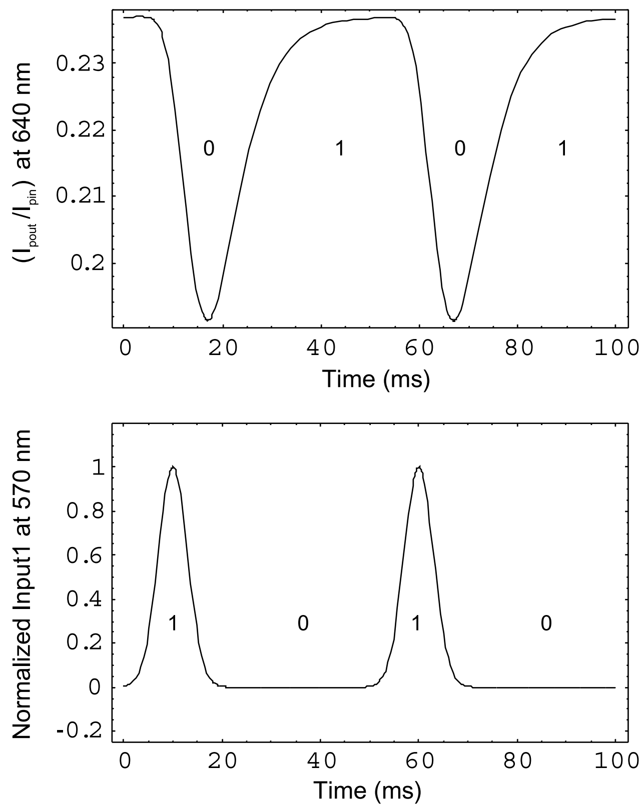

Fig. 3. All-optical inverter (NOT) logic gate (a) Variation of normalized transmitted intensity of the probe beam at 640 nm with time and (b) normalized input pulse profile.

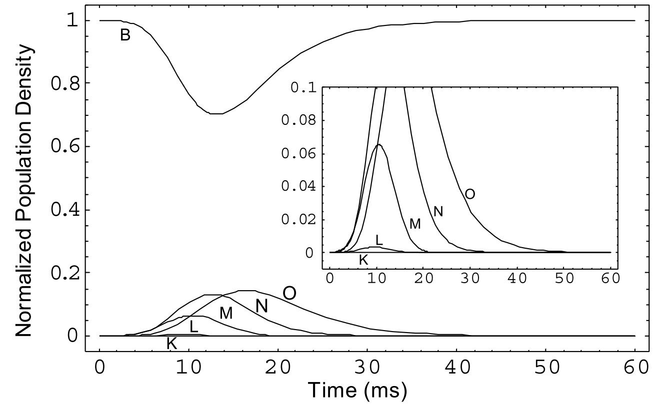

Fig. 4. Variation of normalized population density of B, K, L, M, N, and O states with time. The inset shows a magnified view of the variation for K, L, M, N and O states.

intensity $I'_{m0} = 20$ mW/cm^2. This can be achieved with a 1 nW laser focused to a 5 m^2 spot size.

The variation of the normalized transmitted output intensity of a cw probe laser beam at 640 nm and a pulsed pump laser beam (I'_{m1}) at 570 nm ($I'_{m2} = 0$) with time are shown in Fig. 3(a) and (b) respectively. The transmitted intensity of the probe beam initially high (switch on state) due to lower linear absorption is switched low (switch-off state) when a pulsed laser beam pumps the sample enhancing the population of the O state and increasing the absorption of the probe beam. There is a delay of about 6 ms between the peak of the input and the minimum in the output due to time taken by the molecules to populate the O state. Thus the switching characteristics conform to an all-optical inverter (NOT) logic gate.

Variation in the normalized population density of different intermediate states with time for a single pulse is as shown in Fig. 4. The pump pulse excites the molecules from the initial B state sequentially to other intermediate states, which finally relax to the B state resulting in an increase in its population. There is no appreciable variation in the population of the K state in this time scale as the molecules relax very fast to the L state.

The switching characteristics can be used to design the universal NOR and NAND logic gates with multiple pulsed pump laser beams. Considering two pulsed pump laser beams (I'_{m1} and I'_{m2}) at 570 nm i.e. the two inputs 1 and 2, the output as amplitude modulation of probe laser beam is as shown in Fig. 5(a)–(d). For the all-optical NOR logic gate, the output in this case is low when either one or both the pulses are present and is high when none of the two pulses is present.

The same configuration can also result in an all-optical NAND logic gate if we consider a threshold level as shown by the dashed line in Fig. 5(b). In this case the output can be considered to be high when either one or none of the pulses are present and low only when both the input pulses are present simultaneously.

Variation in the normalized transmission of probe laser beam with time for different pump pulse width values is shown in Fig. 6. As the pulse width (Δt) increases, the switching time and percentage modulation of the probe laser beam increase. The percentage modulation of the probe beam saturates at large Δt values. For instance for $\Delta t = 2$ ms, the switch off and on time are 5 and 19 ms respectively, whereas for $\Delta t = 12$ ms the off and on time are 15 and 30 ms respectively. The percentage modulation for these pulses are 2% and 6% respectively. The symmetry of the curves expectedly increases for Δt greater than the relaxation time of the complete bR photocycle, as this conforms to the steady state case.

The peak pumping intensity required to get the same percentage modulation increases for smaller Δt values. To modulate the output of the probe beam by 21%, the peak pumping intensity required for $\Delta t = 7$ ms, 7 μs and 7 ns is 0.8 W/cm^2, 0.3 kW/cm^2 and 0.2 MW/cm^2 respectively.

The effect of variation in peak pumping intensity (I'_{m0}) on the switching curves is shown in Fig. 7. As I'_{m0} increases, the percentage modulation of the probe laser beam increases. For instance for $I'_{m0} = 20$ mW/cm^2, the probe laser beam is modulated by 5% while for

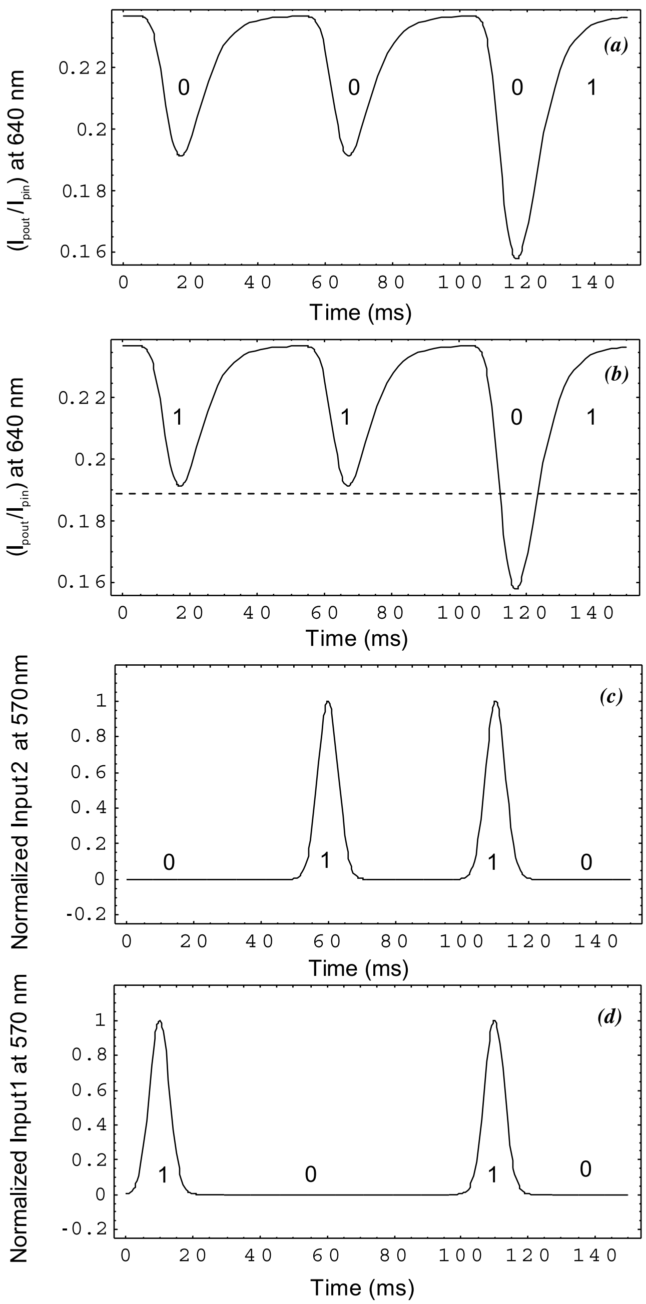

Fig. 5. All-optical logic signals: (a) optical NOR gate function (b) optical NAND gate function (dashed line as the threshold level), both with variation of normalized transmitted intensity of the probe laser beam at 640 nm with time; (c) and (d) are normalized pulse profiles of the two inputs 1 and 2.

$I'_{m0} = 500$ mW/cm^2, it is modulated by 20%. At higher intensity values, the output minima due to single input pulse becomes closer to that due to the presence of both input pulses, thereby reducing the difference between the 1 and 0 state for the NAND case. Hence, NAND logic has to be implemented at relatively lower peak pumping powers.

The effect of variation in the life time of the intermediate O state on the switching characteristics is as

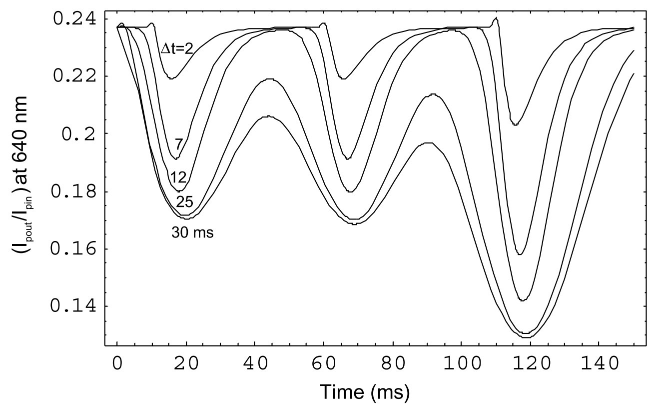

Fig. 6. Variation of normalized transmitted intensity of the probe beam at 640 nm with time, for different pump pulse width (Δt) values.

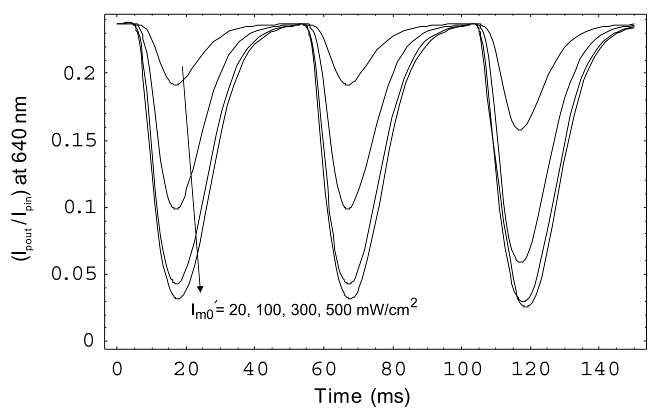

Fig. 7. Variation of normalized transmitted intensity of the probe laser beam at 640 nm with time, for different values of peak pumping intensity (I'_{m0}).

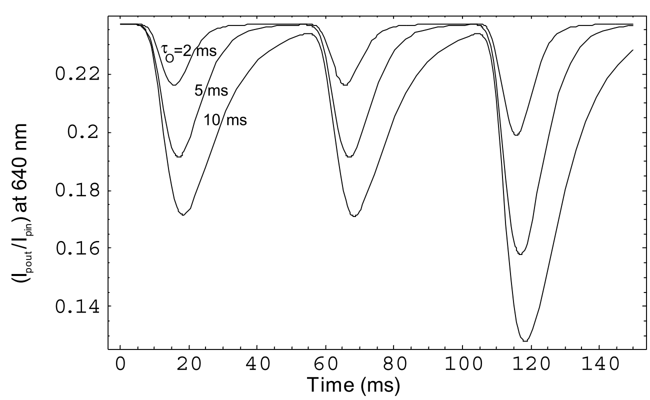

Fig. 8. Variation of normalized transmitted intensity of the probe laser beam at 640 nm with time, for different life time values of O state (τ_O).

shown in Fig. 8. As $\tau_O(1/k_O)$ increases, the switching time increases as the excited molecules relax back to the initial B state in a longer time. An increase in τ_O also increases the population of the O state, hence resulting in an increase in the percentage modulation of the probe laser beam. For $\tau_O = 2$ ms, the switch off and on time

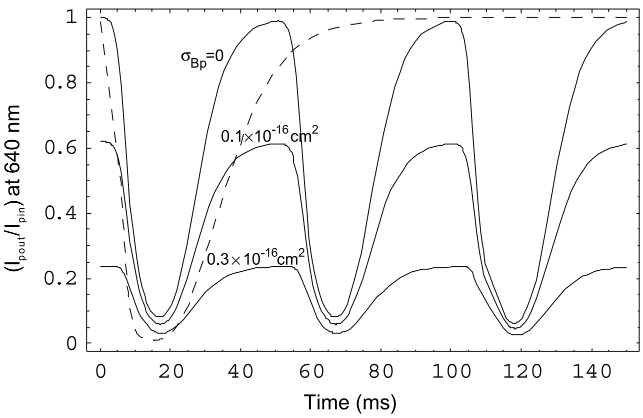

Fig. 9. Variation of normalized transmitted intensity of the probe beam at 640 nm with time, for different absorption cross-section values of B state at probe wavelength (σ_{Bp}), with $I'_{m0} = 500$ mW/cm^2. The dashed line shows 100% modulation for a single pulse with $\sigma_{Bp} = 0$, $\tau_N = 0.3$ ms and $\tau_O = 10$ ms.

are 7 and 18 ms respectively, whereas for $\tau_O = 10$ ms, the off and on time are 12 and 38 ms respectively.

The cross-section value of the initial B state at the probe wavelength is a very sensitive parameter. Variation in the normalized transmitted intensity of the probe laser beam with time for different σ_{Bp} values with $I'_{m0} = 500$ mW/cm^2 is as shown in Fig. 9. As σ_{Bp} decreases, the percentage modulation increases drastically, as it results in an increase in the transmission of the probe beam. For $\sigma_{Bp} = 0.3 \times 10^{-16}$ cm^2 and 0.1×10^{-16} cm^2, the transmittance gets modulated by 20% and 57% respectively. For $\sigma_{Bp} = 0$ initially, the probe beam does not get absorbed at all and as high as 91% modulation of the probe beam can be achieved. The probe beam can be completely switched off (100% modulation) by further increasing the population of O state i.e. increasing τ_O and reducing τ_N, as shown by the dashed line in Fig. 9 for the same peak pump power (500 mW/cm^2) that can be achieved by a 25 nW laser focused to a 5 μm^2 spot size.

The switching time can be reduced by increasing the relaxation rates of the intermediate states so that the excitation time from B → O is reduced and also by decreasing the thermal relaxation time from O → B. A decrease in τ_O results in a decrease in the switching contrast also. The switching contrast can be enhanced by reducing the absorption cross-section of the initial B state at the probe wavelength. The switching time can also be reduced by considering switching of the probe beams corresponding to the peak absorption wavelength of the earlier intermediate states K, L, M or N. The K state is thermally stable at very low temperatures (below 150 K) and the absorption spectra of K, L and N states considerably overlaps with that of the B state, thereby having a large value of σ_{Bp} for probe beams at the respective maximum absorption wavelengths of K, L and N states. For even the M state, $\sigma_{Bp} = 0.5 \times 10^{-16}$ cm^2 i.e. at 412 nm corresponding to the peak absorption of M state, which is larger compared to that for the present case ($\sigma_{Bp} = 0.3 \times 10^{-16}$ cm^2) at 640 nm for the O state. Hence the percentage modulation in the present case is more than that of the other states due to smaller σ_{Bp} and larger reverse saturable absorption at probe wavelength.

Several advantages of the proposed design are noteworthy: (i) the proposed implementation of universal logic gates can be used to realize other logic gates, (ii) all the three logic gates can be realized by using the same configuration by suitably defining the threshold level, (iii) the inputs and output are in digital form, (iv) complete switching (100% modulation) between 0 and 1 states can be achieved, and (v) the operation is at relatively low powers. The switching time of these gates with the typical parameters used for wild type bR is in the ms range. Since the properties of bR can be tailored by physical, chemical and genetic engineering techniques, the switching characteristics and the operation of the logic gates can be optimized for desired applications. Since bR can also be processed as a film or in a crystalline form for 2D/3D applications, bR based NOT gate (all-optical switches) would be potentially useful in applications such as provisioning of light paths in optical cross-connects and add-drop systems in wavelength division multiplexing optical networks. They can provide an alternative to the widely required thermo-optic, MEMS and liquid crystal switches (∼ms range). As large, high-density arrays of these proposed logic gates can also be fabricated that can operate at very low switching energies with high thermal stability, they would be useful in parallel optical computing.

4. Conclusion

We have demonstrated implementation of all-optical NOT, and the universal NOR and NAND logic gates with bR based on all-optical switching of a cw probe laser beam by multiple pulsed laser beams, considering a six state model of its photocycle. All three logic functions can be implemented in bR with the same configuration by adjusting the output threshold level. The effect of variation in pump pulse width, peak pumping intensity, life time of the O state and absorption cross-section of B state at probe wavelength on the switching characteristics have also been shown. The proposed all-optical logic gates would be useful due to advantages of small size, simple and low power operation, small linear absorption coefficient, mirror-less structure, and flexibility in design.

Acknowledgements

The authors are grateful to the All India Council for Technical Education and the Department of Science and

Technology, Govt. of India for partial support of this work.

References

[1] D.J. Bishop, C.R. Giles, S.R. Das, Sci. Am. 284 (2001) 88.
[2] S. Roy, C.P. Singh, K.P.J. Reddy, Appl. Phys. Lett. 77 (2000) 2656.
[3] N. Hampp, Chem. Rev. 100 (2000) 1755.
[4] R.R. Birge, N.B. Gillespie, E.W. Izaguirre, A. Kusnetzow, A.F. Lawrence, D. Singh, Q.W. Song, E. Schmidt, J.A. Stuart, S. Seetharaman, K.J. Wise, J. Phys. Chem. B 103 (1999) 10746.
[5] A. Royant, E. Edman, E.P. Peyroula, E.M. Landau, R. Neutze, Nature (London) 406 (2000) 645.
[6] H. Luecke, Biochimica et Biophysica Acta 1460 (2000) 133.
[7] J.K. Lanyi, A. Pohorille, Trends Biotechnol. 19 (2001) 140.
[8] L. Keszthelyi, P. Ormos, G. Varo, G. Groma, IEEE EMBS 12 (1990) 1712.
[9] B.L. Yao, D.L. Xu, X. Hou, K.S. Hu, A.J. Wang, J. Appl. Phys. 89 (2001) 797.
[10] P.C. Pandey, B.C. Upadhyay, C.M.D. Pandey, H.C. Pathak, Sens. Actuat. B 56 (1999) 112.
[11] H. Takei, A. Lewis, Z. Chen, I. Nebenzahl, Appl. Opt. 30 (1992) 500.
[12] F.T. Hong, Molecular and biomolecular electronics, in: R.R. Birge (Ed.), Advances in Chemistry Series 240, American Chemical Society, Washington DC, 1994.
[13] N. Hampp, R. Thoma, D. Zeisel, C. Brauchle, Adv. Chem. 240 (1994) 511.
[14] J.D. Downie, D.A. Timucin, D.T. Smithey, M. Crew, Opt. Lett. 23 (1998) 730.
[15] N. Hampp, Opt. Lett. 26 (2001) 1702.
[16] J.Y. Huang, Z. Chen, A. Lewis, J. Phys. Chem. 93 (1989) 3314.
[17] O. Werner, B. Fisher, A. Lewis, I. Nebenzahl, Opt. Lett. 15 (1990) 1117.
[18] R. Thoma, N. Hampp, C. Brauchle, D. Oesterhelt, Opt. Lett. 16 (1991) 651.
[19] D.V.G.L.N. Rao, F.J. Aranda, B.I. Wiley, J.A. Akkara, D.L. Kaplan, J.F. Roach, Appl. Phys. Lett. 63 (1993) 1489.
[20] K.P.J. Reddy, Appl. Phys. Lett. 64 (1994) 2776.
[21] Q.W. Song, C. Zhang, R. Blumer, R.B. Gross, Z. Chen, R.R. Birge, Opt. Lett. 18 (1993) 1373.
[22] K.P.J. Reddy, J. Appl. Phys. 77 (1995) 6108.
[23] H. Takei, N. Shimizu, Appl. Opt. 35 (1996) 1848.
[24] S. Roy, K.P.J. Reddy, Curr. Sci. 78 (2000) 184.
[25] J. Joseph, F.J. Aranda, D.V.G.L.N. Rao, J.A. Akkara, M. Nakashima, Opt. Lett. 21 (1996) 1499.
[26] D.P. Shelton, Opt. Lett. 22 (1997) 1728.
[27] H. Imam, L.P. Lindvold, P.S. Ramanujam, Opt. Lett. 20 (1995) 225.
[28] D. Sanchez-de-la-Llave, M.A. Fiddy, Appl. Opt. 38 (1999) 815.
[29] M. Sanio, U. Settele, K. Anderle, N. Hampp, Opt. Lett. 24 (1999) 379.
[30] A. Lewis, Y. Albeck, Z. Lange, J. Benchowaski, G. Weizman, Science 275 (1997) 1462.
[31] R.R. Birge, Sci. Am. 272 (1995) 90.
[32] D.V.G.L.N. Rao, F.J. Aranda, D.N. Rao, Z. Chen, J.A. Akkara, D.L. Kaplan, M. Nakashima, Opt. Commun. 127 (1996) 193.
[33] L.Q. Gu, C.P. Zhang, A.F. Niu, J. Li, G.Y. Zhang, Y.M. Wang, M.R. Tong, J.L. Pan, Q.W. Song, B. Parson, R.R. Birge, Opt. Commun. 131 (1996) 25.
[34] T. Zhang, C. Zhang, G. Fu, Y. Li, L. Gu, G. Zhang, Q.W. Song, B. Parsons, R.R. Birge, Opt. Eng. 39 (2000) 527.
[35] R.E. De Araujo, G. Borissevitch, A.S.L. Gomes, Electron. Lett. 36 (2000) 71.
[36] K. Clays, S.V. Elshocht, M. Chi, E. Lepoudre, A. Persoons, J. Opt. Soc. Am. B 18 (2001) 1474.
[37] C. Li, L. Zhang, R. Wang, Y. Song, Y. Wang, J. Opt. Soc. Am. B 11 (1994) 1356.
[38] F.Z. Henari, K.H. Cazzini, D.N. Weldon, W.J. Blau, Appl. Phys. Lett. 68 (1996) 629.
[39] F.Z. Henari, J. Opt. A: Pure Appl. Opt. 3 (2001) 188.
[40] R.W. Hendler, R.I. Shrager, S. Bose, J. Phys. Chem. B 105 (2001) 3319.
[41] T. Kobayashi, T. Saito, H. Ohtani, Nature (London) 414 (2001) 531.
[42] S. Roy, C.P. Singh, K.P.J. Reddy, J. Appl. Phys. 90 (2001) 3679.